ORIGINAL PAPER

Solid electrolyte interphase formation on metallic lithium

**Andrzej Lewandowski · Agnieszka Swiderska-Mocek ·
Lukasz Waliszewski**

Abstract Solutions of three salts (LiBF$_4$, LiNTf$_2$, LiPF$_6$) in
N-methyl-2-pyrrolidone (NMP), selected arbitrarily as a ref-
erence solvent, were investigated by electrochemical imped-
ance spectroscopy (EIS) and scanning electron microscopy
techniques. The lithium surface in contact with LiPF$_6$ in
NMP electrolyte was covered with a protective layer (SEI)
which morphology comprise small particles (of ca. 0.2 μm
in radius). This salt was selected for further studies. The
impedance of the Li|(LiPF$_6$ in NMP+additive)|Li system
was measured immediately after cell assembly and after
galvanostatic charging/discharging. Fifteen different addi-
tives (10 wt.%) were used. The efficiency of individual
additives was evaluated in terms of the Li|electrolyte system
resistance (ΔR) or total cell impedance reduction, both
deduced from EIS. Some of the additives were able to form
the SEI layer and to reduce resistance/impedance of the Li|
electrolyte interphase. In such cases, the lithium surface was
covered with relatively uniform conglomerates, or regions
separated by cracks, of ca. 1–2 μm in dimension.

Keywords Lithium · SEI · Electrolyte additive · EIS

Introduction

Both lithium-metal and lithiated graphite anodes applied in
lithium or Li-ion batteries react with electrolytes with the
formation of a passivation layer, usually called the solid
electrolyte interphase (SEI), protecting them against further

corrosion [1, 2]. Cyclic carbonates, typically used as com-
ponents (solvents) of lithium electrolytes, react with Li or
C$_6$Li anodes with the formation of Li$^+$ conducting SEI
[3–8]. The SEI layer is responsible for the chemical and
electrochemical stability of electrodes. However, SEI form-
ing cyclic carbonates are volatile and hence, the system is
flammable (during overheating, overcharging, or mechani-
cal damage). Therefore, for safety reasons, all components
of a Li-ion battery, including the electrolyte, should be char-
acterised by non-flammability. The non-volatility of room
temperature ionic liquids is important from the point of view
of their possible application as non-flammable electrolytes in
lithium and Li-ion batteries [9–12]. Another approach is to
find a low vapour pressure molecular solvent, for example γ-
butyrolactone (γ-BL, T_b=205 °C) [13] or tetramethylene
sulfone (TMS, T_b=280 °C) [14]. However, unconventional
systems, such as ionic liquids and high boiling point solvents
(γ-BL, TMS) do not form SEI protective layer but rather
resistive corrosion products. Therefore, in non-classical elec-
trolytes additives are necessary to improve Li and Li-ion
battery performance [6, 15]. The general aim of the present
study was to provide visual (scanning electron microscopy,
SEM) and quantitative (electrochemical impedance spectros-
copy, EIS) comparison of additives in an arbitrarily selected
solvent (N-methyl pyrrolidone). The effect of the additive
presence on the Li|electrolyte impedance may be used as a
measure of its SEI forming properties.

Experimental

Materials

Lithium foil (0.75 mm thick, Aldrich), lithium hexafluoro-
phosphate (LiPF$_6$, battery grade >99 %, Fluka), vinylene

A. Lewandowski (✉) · A. Swiderska-Mocek · L. Waliszewski
Faculty of Chemical Technology,
Poznan University of Technology,
60965 Poznan, Poland
e-mail: andrzej.lewandowski@put.poznan.pl

carbonate (VC, >97 %, Aldrich), vinyl ethylene carbonate (VEC, >99 %, Aldrich), ethylene carbonate (EC, anhydrous 99 %, Aldrich), propylene carbonate (PC, anhydrous 99,7 %, Aldrich), dimethyl carbonate (DMC, anhydrous >99 %, Aldrich), diethyl carbonate (DEC, anhydrous >99 %, Aldrich), ethylene sulphite (ES, 98 %, Aldrich), vinyl acetate (Vac, >99 %, Fluka), gamma-butyrolactone (γ-BL, >99 %, Aldrich), triphenyl phosphate (TPhPh, Aldrich), phenyl isocyanate (PhIsCy, >99 %, Fluka), methyl cinnamate (MCin, >99 %, Aldrich), dimethyl sulfoxide (DMSO, Merck), and styrene (>99 %, Aldrich) were used as received. Electrolyte was obtained by dissolution of the solid $LiPF_6$ salt in N-methyl-2-pyrrolidone (NMP, Fluka) (1 M solution of $LiPF_6$ salt in NMP). Electrolytes were prepared in a dry argon atmosphere in a glove box. They contained various additives (VC, VEC, EC, PC, DMC, DEC, ES, Vac, γ-BL, TPhPh, PhIsCy, MCin, DMSO, styrene) at 10 wt.%.

Measurements

The performances of the cells were characterized using electrochemical impedance spectroscopy (EIS) and using galvanostatic charge-discharge tests. The Li/electrolyte/Li cells were assembled in a dry argon atmosphere in a glove box. Two lithium foils were separated by the glass micro-fibre GF/A separator (Whatman), placed in an adopted 0.5" Swagelok® connecting tube. Interface resistance at the electrode/electrolyte interphase was measured using an ac impedance analyzer (Atlas—Sollich system, Poland). The Li/electrolyte/Li cells were polarised with a constant current (1 mA) for 45 min and for the next 45 min in the opposite direction. Scanning electron microscopy (SEM) of the lithium electrode was performed with the Tescan Vega 5153 apparatus. After electrochemical measurements, cells were disassembled, electrodes washed with DMC and dried in vacuum at room temperature. All operations were performed in a dry argon atmosphere in a glove box.

Results

Salt effect

Figure 1 shows impedance spectra of the Li|NMP+LiX|Li system (LiX=$LiBF_4$, $LiNTf_2$, $LiPF_6$) taken immediately after the cell assembling and after its galvanostatic charging/discharging. In the case of all salts, the impedance of the system increased after the electrochemical SEI formation. The impedance of the fresh system (without galvanostatic polarisation) may be interpreted as a result of lithium reaction with the electrolyte (solvent and salt) with the formation of a passivation layer. The highest impedance is characteristic
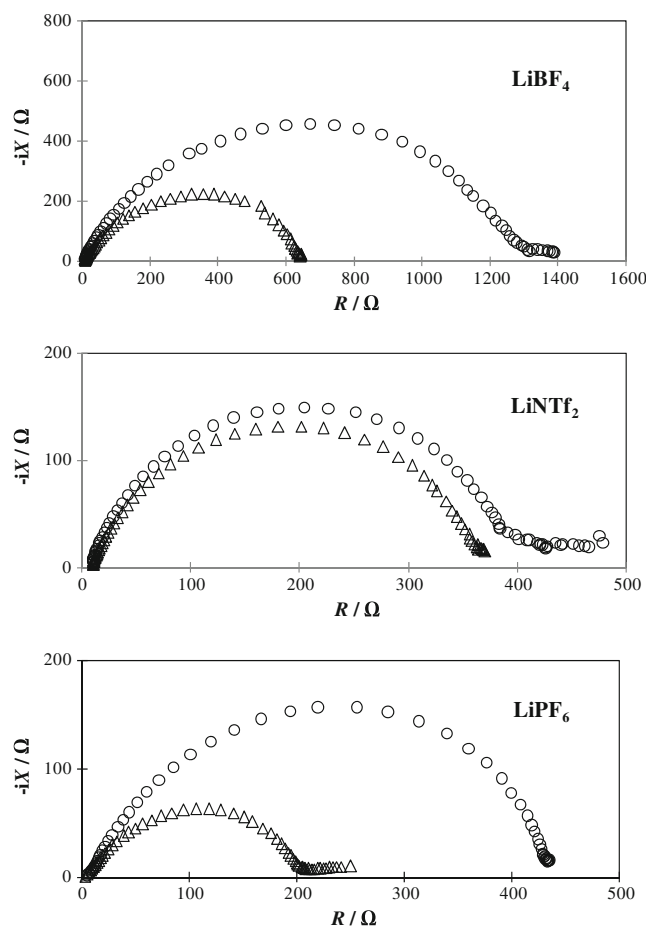

Fig. 1 Impedance spectra of the Li|NMP + LiX|Li system taken immediately after cell assembling ($\triangle$) and after its galvanostatic charging/discharging (o). Current, 1 mA cm^{-2}, charging/discharging time, 45 min. LiX stands for $LiBF_4$, $LiNTf_2$ or $LiPF_6$

of the Li|($LiBF_4$ in NMP) system (of the order of 600 Ω referred to 1 cm^2 of the lithium geometrical surface area). In the case of the solutions of the other salts ($LiNTf_2$ or $LiPF_6$), it is lower (ca. 400 and 200 Ω, respectively). During the electrochemical charging/discharging, the passivation layer is modified as a result of (1) the thickness, (2) composition (solid lithium salts and polymers), (3) and morphology changes. As a result of the lithium/electrolyte interphase modification, the total resistance (impedance) also changes. In the case of $LiBF_4$ and $LiPF_6$ salts, the total impedance increases by ca. 100 %. The corresponding value for $LiNTf_2$ salt is much smaller. SEM images of lithium metal surface covered with corrosion products after a chemical reaction with the NMP+LiX electrolyte (without electrochemical charging/discharging) are shown in Fig. 2. It can be seen that metallic lithium, after its contact with NMP solutions of $LiBF_4$ and $LiNTf_2$ salts, reacts with the formation of a uniform passivation film. In the case of the $LiPF_6$ in NMP electrolyte, the lithium surface is covered with small particles (of ca. 0.2 μm in radius). This may suggest that in the case of Li|($LiPF_6$ in NMP), the specific
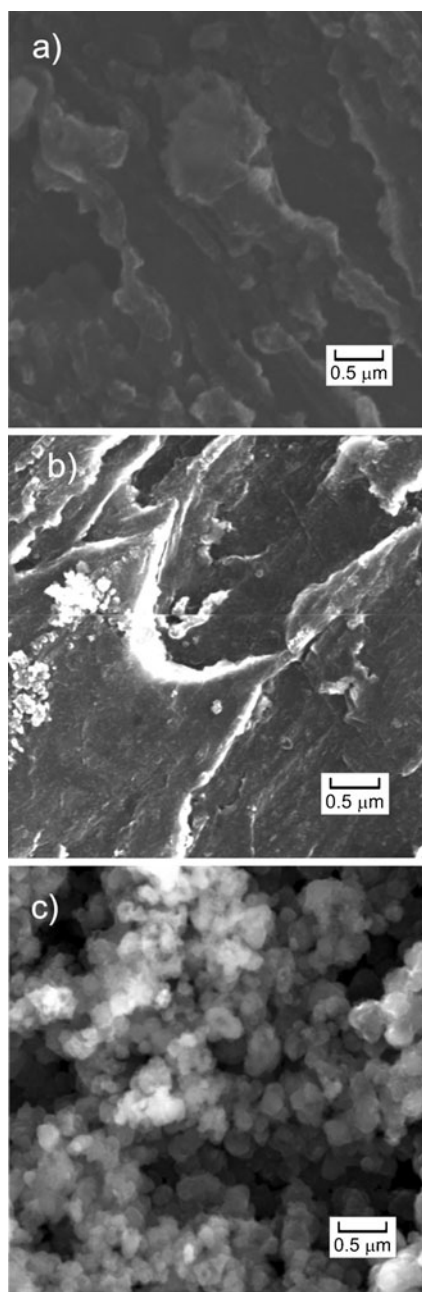
Fig. 2 SEM images of lithium metal surface covered with corrosion products after chemical reaction with NMP + LiX electrolyte (without electrochemical charging/discharging) (**a**) NMP + 1 M LiBF$_4$; (**b**) NMP + 1 M LiNTf$_2$ and (**c**) NMP + 1 M LiPF$_6$. Magnification, 13,000×

morphology (particles instead of the film layer) is due to the formation of Li salt solid particles (for example LiF) surrounded by a polymer film [3, 16–18].

Additives

Impedance spectra of Li|NMP+LiPF$_6$+VC (10 wt.%)|Li and Li|NMP+LiPF$_6$+Vac (10 wt.%)|Li are shown in Fig. 3. It can be seen that the impedance taken immediately

after cell assembly is higher in comparison to that characteristic of the electrochemically cycled cell (1 charging and 1 discharging cycle). This suggests that electrochemically prepared SEI is more conductive in comparison to the spontaneously formed passivation films. The ohmic resistance values of the freshly prepared Li|electrolyte systems were ca. 120 and 300 Ω for VC and Vac as additives, respectively. SEI resistance (after charging/discharging) is considerably lower (ca. 80 Ω for VC and ca. 50 Ω for Vac). In contrast to such a behaviour, in some cases, the electrochemical charging/discharging led to an increase in the total system impedance. The Li|NMP+LiPF$_6$+ES (10 wt.%)|Li and Li|NMP+LiPF$_6$+ES (10 wt.%)|Li systems may serve as examples. Here, the ohmic resistance increased to 220 Ω (PC) or even 300 Ω (ES) (Fig. 4). All impedance spectra consist of a flat 'semicircle', usually followed by a short linear part at a low frequency region. The high and medium frequency part may be approximated by a semi-ellipse rather than the semi-circle, as its major radius (the real axis R) does not equal the minor radius (the imaginary axis—iX). Typically, the value (expressed in ohms) of the major radius is higher than the corresponding value of the minor radius ($R^2 > (iX)^2$). This may suggest that the semi-elipse is a superposition of two semi-circles, representing two RC elements in a series, due to the SEI formation and a charge transfer process (Fig. 5). The frequency range of the linear-part is relatively narrow and the slope is much below 45°. The linear, low-frequency part, obtained for the reduction of Li$^+$ on the metal-lithium anode is different from that characteristic of graphite anodes, where the
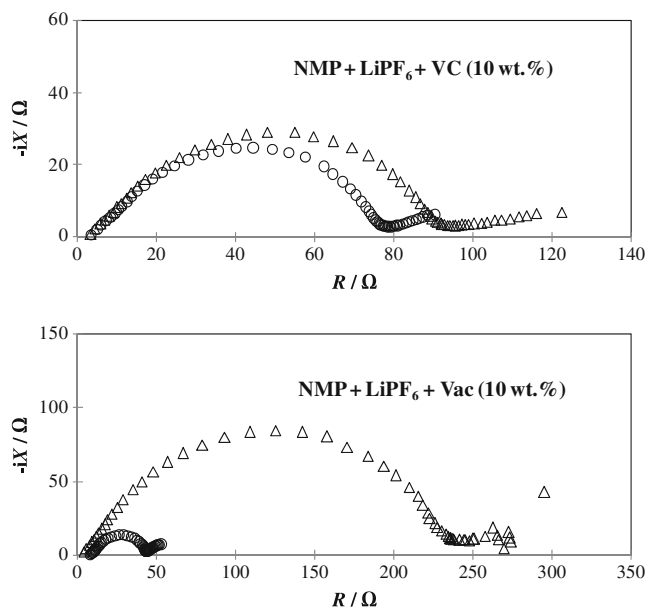

Fig. 3 Impedance spectra of Li|NMP + LiPF$_6$ + VC (10 wt.%)|Li and Li|NMP + LiPF$_6$ + Vac (10 wt.%)|Li cells taken immediately after cell assembling (△) or after its galvanostatic charging/discharging (o). Current, 1 mA cm^{-2}, charging/discharging time, 45 min
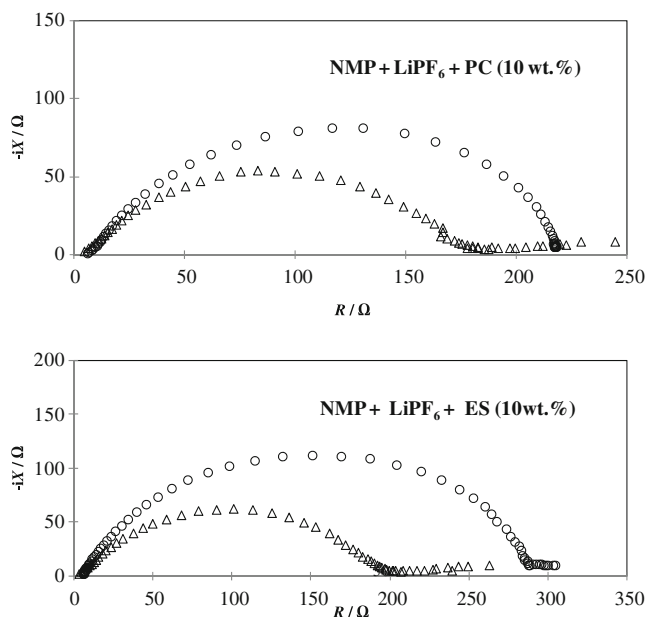
Fig. 4 Impedance spectra of Li|NMP + LiPF$_6$ + PC(10 wt.%)|Li and Li|NMP + LiPF$_6$ + ES(10 wt.%)|Li cells taken immediately after cell assembling (Δ) or after its galvanostatic charging/discharging (o). Current, 1 mA cm^{-2}, charging/discharging time, 45 min

Warburg impedance is predominant due to lithium diffusion in solid graphite [19]. This may suggest that low-frequency linear parts of impedance spectra shown in Figs. 1, 3, 4 and 8 cannot be described by the Warburg element Z_W, but rather by an element Z (without ascribing any physical meaning). However, commercial software packages used for impedance data deconvolution generally contain the Z_W element for the description of the low frequency region. Due to the fact that the low frequency part of impedance plots measured for the Li-metal|Li$^+$ systems does not exhibit a Warburg-like nature, two attempts for experimental plot deconvolution were made. First, the data measured in the whole frequency region were analysed with $Z=Z_W$. In the second attempt, both the low frequency region data (the linear part of spectra) and the Z element in the equivalent circuit were excluded from the fitting procedure. Both attempts led to very similar R_{SEI} and R_{ct} values. In addition, standard deviations of calculated and experimental impedances were comparable. Total impedances (Imp), measured at a frequency of 0.1 Hz, before and after galvanostatic charging/discharging of Li|NMP+LiPF$_6$+additive (10 wt.%)|Li systems, for 15 additives studied, are
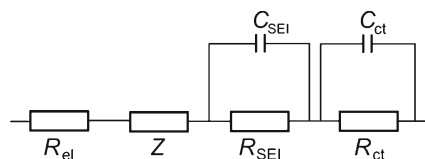

Fig. 5 An equivalent circuit representing the Li/electrolyte system

summarised in Table 1. Values of SEI ohmic resistance R_{SEI} and charge transfer resistance R_{ct}, obtained from the deconvolution procedure, are also shown in Table 1. Total impedance (Imp) measured at a low frequency of 0.1 Hz immediately after the Li|electrolyte|Li cell assembling, is typically of the order of 200–300 Ω. In the case of the VC containing electrolyte, its value is lower (120 Ω) while electrolytes based on EC and Vac+VC additives show considerably higher impedance (ca. 600 Ω). After galvanostatic charging/discharging, the total impedance decreases (VC, EC, PC, γ-BL, TPhPh, PhIsCy, Vac, Vac+VC) or increases (DEC, DMC, VEC, DMSO, ES, MCin, styrene). The electrochemical SEI formation led to the lowest total impedance in the case of VC (91 Ω) and Vac (53 Ω). On the other hand, in the case of styrene as the additive, the electrochemical treatment resulted in impedance increasing up to 613 Ω (from an initial value of 239 Ω). A similar decrease of the $R_{SEI}+R_{ct}$ ohmic resistance drop after electrochemical charging/discharging ($\Delta R=(R_{SEI}+R_{ct})_{after}-(R_{SEI}+R_{ct})_{before}$) for cells with electrolytes containing the same additives (except PC) was observed (Table 1). Negative ΔImp or ΔR values suggest a replacement of the less conductive passivation layer by electrochemically formed SEI. Figures 6 and 7 show examples of SEM images of the lithium layer after electrochemical SEI formation from electrolytes (NMP+LiPF$_6$) containing additives reducing (VC and Vac, Fig. 6) or increasing (PC and ES , Fig. 7) ohmic resistance. While the metallic lithium in the NMP+LiPF$_6$ electrolyte is covered with spherical particles (Fig. 2c), the SEI structure (formed electrochemically, shown in Figs. 6 and 7) is different. In the case of VC as the additive, the lithium surface is covered with smooth and uniform regions, separated by cracks, of ca. 1–2 μm in dimension, one order of magnitude higher in comparison to that characteristic of spherical particles formed without VC. On the other hand, the morphology of the SEI structure formed in the presence of Vac was a foamlike, organised in conglomerates of a comparable dimension (1–2 μm). A similar morphology may be observed in the case of PC and ES as additives. Ohmic resistance in the case of PC as the additive increases after galvanostatic charging/discharging ($\Delta R>0$), but the corresponding total impedance change is negative (ΔImp<0). In all the other cases negative ΔR corresponds to negative ΔImp values. While the electrochemical pre-treatment of the Li|electrolyte system resulted always in the formation of the more uniform morphology, the corresponding impedance increased or decreased. In general, electrochemical SEI formation results in a morphology change from spherical (0.2 μm) into a more uniform system (1–2 μm). This effect was observed before for the graphite [17, 18] and silicone [16] anodes. The passivation layer formed in a classical LiPF$_6$ solution in EC+DMC electrolyte without any additive was non-homogeneous and embedded with spherical particles, which were assumed to be LiF crystals. SEM images of the SEI layer formed on the graphite and

Table 1 Total Li|NMP + LiPF$_6$ + additive (10 wt.%)|Li cell impedance (Imp), together with corresponding resistances of the SEI layer (R_{SEI}) and charge transfer process (R_{ct}), measured before and after its electrochemical formation (galvanostatic charging/discharging) (lithium electrodes surface area, 1 cm^2)

Additives	Before charge/discharge [Ω]			After charge/discharge [Ω]			Difference [Ω]	
	R_{SEI}	R_{ct}	Imp	R_{SEI}	R_{ct}	Imp	ΔR[a]	ΔImp[b]
–	41	149	250	27	363	430	200	180
10 % VC	35	53	123	24	47	91	−17	−32
10 % DEC	46	83	171	48	160	225	79	54
10 % DMC	44	136	188	100	240	379	160	191
10 % EC	129	275	569	68	235	326	−101	−243
10 % PC	46	118	245	48	161	217	45	−28
10 % VEC	30	152	271	25	366	411	209	140
10 % γ-BL	29	152	287	10	126	147	−45	−140
10 % DMSO	23	146	246	39	243	280	113	34
10 % ES	39	143	263	63	214	305	95	42
10 % TPhPh	80	157	253	32	137	185	−68	−68
10 % PhIsCy	79	113	253	56	77	170	−59	−83
10 % MCin	26	139	241	39	367	310	241	69
10 % Vac	26	188	273	7	32	53	−175	−220
5 % Vac + 5 % VC	166	225	671	93	183	310	−115	−361
10 % styrene	22	80	239	111	350	613	359	374

[a] $\Delta R = \sum R_{after} - \sum R_{before}$ (difference in total resistance, measured before and after electrochemical polarization)

[b] ΔImp = Imp$_{after}$ − Imp$_{before}$ (difference of impedance at 0.1 Hz, measured before and after electrochemical polarization)

Imp is total system impedance

silicone in electrolytes containing VC showed rather a smooth and uniform morphology [16–18]. Generally, the microscopic techniques (SEM) show changes in the surface morphology, but do not provide information on the layer impedance. In the case of all additives tested, the spherical-like particles were transformed (during galvanostatic charging/discharging) into much more uniform structures. However, the ohmic resistance or total system impedance may increase or decrease. Therefore, the resistance/impedance decrease may serve as the criterion of the anode (lithium) surface improvement from the point of view of its ability to conduct Li$^+$ cations through the SEI layer before the charge transfer reaction. The efficiency of additives, from the point of view of reducing metallic-lithium resistance (ΔR), suggested by EIS analysis is the following: Vac>Vac+VC>EC>TPhPh>PhIsCy>γ-BL> VC. The other compounds did not show any improvement (decrease) of the Li|(LiPF$_6$ in NMP) system resistance (impedance). This is difficult to compare these results with literature data due to the variety of solvents, salts and electrochemical conditions applied. In addition, there are very few works testing metallic-lithium [20–22], while in the case of the graphite anode, there are numerous studies. In the latter case attention is focused on charging/discharging efficiency [23–29], SEM observations of the graphite surface [8, 14, 23–25, 27, 29–31] and EIS analysis [23, 24, 29, 30, 32–35].

In addition, in some papers, only the LiC$_6$ anode was studied [11, 23–25, 27–30], while in others, the complete cell was tested [13, 36–41]. The additives improving Li and LiC$_6$ performance were usually tested in electrolytes based on cyclic carbonates or carbonate mixtures, exhibiting SEI forming properties by themselves. However, in the case of ionic liquids as electrolytes, additives seem to be necessary for the functioning of anodes or the Li-ion cell [9–12, 24–28, 30, 39, 42–44]. Among compounds tested, VC seems to be the most popular and effective additive.

Impedance changes with time

Independently of the additive used, ohmic resistance of the SEI layer increases with time (Fig. 8). Evolution of the Li| NMP+LiPF$_6$+VC(10 wt.%)|Li cell impedance, measured for the system without electrochemical SEI formation can be seen on Fig. 8a. The ohmic resistance measured immediately after the cell assembling was ca. 120 Ω and the corresponding reactance was ca. 30 Ω. During cell storage, the total impedance increased with time by one order of magnitude; ohmic resistance to ca. 2 kΩ and reactance to ca. 600 Ω (after 12 days). In the case of the same cell with the SEI layer formed electrochemically, the impedance evolution was considerably smaller (Fig. 8b): ohmic resistance
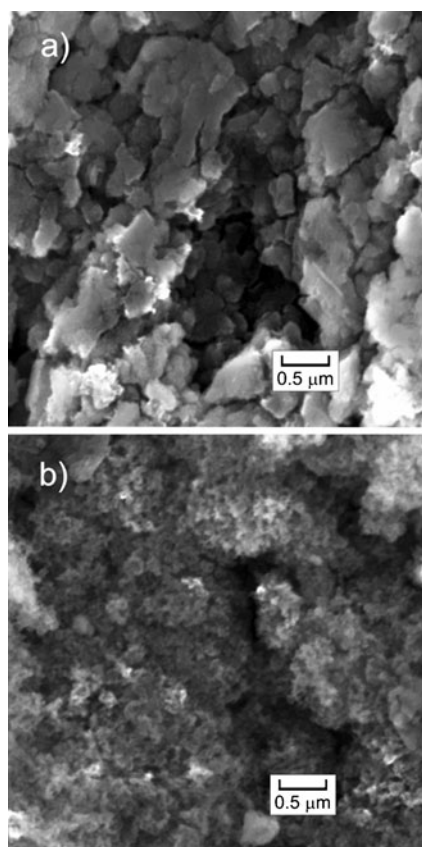
Fig. 6 SEM images of lithium metal surface after its electrochemical charging/discharging in electrolytes containing additives: NMP + 1 M LiPF$_6$ + additive(10 wt.%); (**a**) VC, (**b**) Vac. Magnification, 13,000×

Fig. 7 SEM images of lithium metal surface after its electrochemical charging/discharging in electrolytes containing additives: NMP + 1 M LiPF$_6$ + additive(10 wt.%); (**a**) PC, (**b**) ES. Magnification, 13,000×

increased to ca. 400 Ω and reactance to ca. 130 Ω (after 13 days). This indicates that the electrochemical formation of SEI protects the Li|electrolyte system against its aging (demonstrated as the total impedance increase).

Conclusions

1. Solutions of three salts (LiBF$_4$, LiNTf$_2$, LiPF$_6$) in NMP (not forming SEI layer), selected arbitrarily as a reference solvent, were investigated by EIS and SEM techniques. The lithium surface in contact with the LiPF$_6$ in NMP electrolyte was covered with small particles (of ca. 0.2 μm in radius).

2. The Li|(LiPF$_6$ in NMP+additive)|Li impedance taken immediately after cell assembling and after galvanostatic charging/discharging showed differences in ohmic resistance and total impedance. The presence of the following additives: Vac, Vac+VC, EC, TPhPh, PhIsCy, γ-BL, VC resulted in a decrease of Li|electrolyte resistance. The other tested compounds (DEC, DMC, PC, EC, DMSO, ES, MCin, styrene) did not show any reduction of the resistance (impedance).
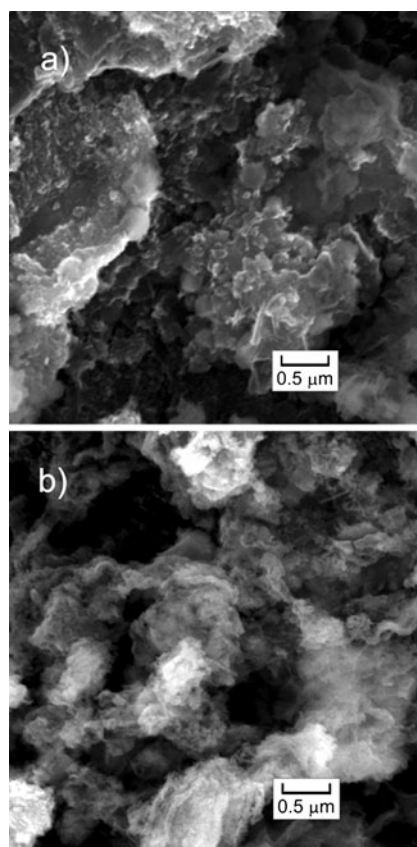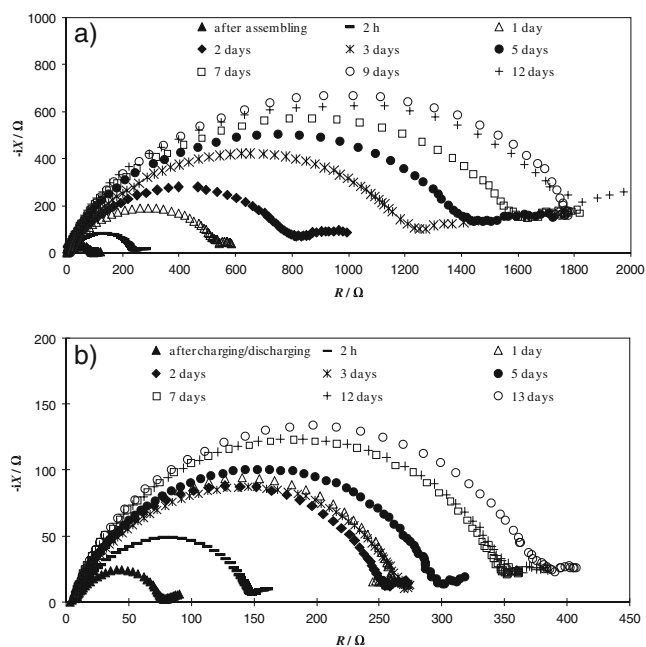

Fig. 8 Impedance evolution of the Li|NMP + LiPF$_6$ + VC (10 wt.%)| Li cell as a function of storage time: (**a**) Li without SEI (**b**) Li protected by SEI formed electrochemically. The system was kept under open circuit conditions

3. In the case of the SEI forming additives, the lithium surface was covered with relatively uniform regions or conglomerates, separated by cracks, of ca. 1–2 μm in dimension (SEI layer).

4. The electrochemical formation of SEI protects the Li| electrolyte system against its aging (the resistance and total impedance evolution with time is much smaller).

References

1. Wakihara M, Yamamoto O (1998) Lithium ion batteries. Wiley-VCH, Weinheim
2. Scrosati B, Garche J (2010) J Power Sources 195:2419–2430
3. Aurbach D (2000) J Power Sources 89:206–218
4. Aurbach D (2002) In: van Schalkwijk WA, Scrosati B (eds) Advances in lithium-ion batteries. Kluwer, New York
5. Edström K, Herstedt M, Abraham DP (2006) J Power Sources 153:380–384
6. Zhang SS (2006) J Power Sources 162:1379–1394
7. Aurbach D, Markovsky B, Salitra G, Markevich E, Taluossef Y, Koltypin M, Nazar L, Ellis B, Kovacheva D (2007) J Power Sources 165:491–499
8. Verma P, Maire P, Novak P (2010) Electrochim Acta 55:6332–6341
9. Webber A, Blomgren GE (2002) In: van Schalkwijk AW, Scrosati B (eds) Advances in lithium-ion batteries. Kluwer, New York
10. Galinski M, Lewandowski A, Stepniak I (2006) Electrochim Acta 51:5567–5580
11. Lewandowski A, Swiderska-Mocek A (2009) J Power Sources 194:601–609
12. Guerfi A, Dontigny M, Charest P, Petitclerc M, Lagace M, Vijh A, Zaghib K (2010) J Power Sources 195:845–852
13. Kinoshita SC, Kotato M, Sakata Y, Ue M, Watanabe Y, Morimoto H, Tobishima SI (2008) J Power Sources 183:755–760
14. Lewandowski A, Kurc B, Stepniak I, Swiderska-Mocek A (2011) Electrochim Acta 56:5972–5978
15. Xu K (2004) Chem Rev 104:4303–4417
16. Chen L, Wang K, Xie X, Xie J (2007) J Power Sources 174:538–543
17. Buqa H, Golob P, Winter M, Besenhard JO (2001) J Power Sources 97–98:122–125
18. Andreson AM, Edström K (2001) J Electrochem Soc 148:A1100–A1109
19. Lewandowski A, Acznik I (2010) Electrochim Acta 56:211–214
20. Xiong S, Kai X, Hong X, Diao Y (2011) Ionics. doi:10.1007?s11581-011-0628-1
21. Umeda GA, Menke E, Richard M, Stamm KL, Wudl F, Dunn B (2011) J Mater Chem 21:1593–1599
22. Ding F, Hu X, Liu Y (2007) Journal of Wuhan University of Technology-Mater Sci Ed 22:494–498
23. Chang CC, Hsu SH, Jung YF, Yang CH (2011) J Power Sources 196:9605–9611
24. Zheng H, Jiang K, Abe T, Ogumi Z (2006) Carbon 44:203–210
25. Holzapfel M, Jost C, Novak P (2004) Chem Commun 2098-2099
26. Sun HG, Dai S (2010) Electrochim Acta 55:4618–4626
27. Holzapfel M, Jost C, Prodi-Schwab A, Krumeich F, Wursig A, Buqa H, Novak P (2005) Carbon 43:1488–1498
28. Lux SF, Schmuck M, Jeong S, Passerini S, Winter M, Balducci A (2010) Int J Energy Res 34:97–106
29. Zheng H, Li B, Fu Y, Abe T, Ogumi Z (2006) Electrochim Acta 52:1556–1562
30. Fu Y, Chen C, Qiu C, Ma X (2009) J Appl Electrochem 39:2597–2603
31. Abe K, Miyoshi K, Hattori T, Ushigoe Y, Yoshitake H (2008) J Power Sources 184:449–455
32. Lee HH, Wang YY, Wan CC, Yang MH, Wu HC, Shieh DT (2005) J Appl Electrochem 35:615–623
33. Itagaki M, Yotsuda S, Kobari N, Watanabe K, Kinoshita S, Ue M (2006) Electrochim Acta 51:1629–1635
34. Ota H, Sato T, Suzuki H, Usami T (2001) J Power Sources 97–98:107–113
35. Itagaki M, Kobari N, Yotsuda S, Watanabe K, Kinoshita S, Ue M (2005) J Power Sources 148:78–84
36. Sun X, Angell CA (2009) Electrochem Commun 11:1418–1421
37. Shim EG, Nam TH, Kim JG, Kim HS, Moon SI (2007) Electrochim Acta 53:650–656
38. Shim EG, Nam TH, Kim JG, Kim HS, Moon SI (2007) J Power Sources 172:901–907
39. Sato T, Maruo T, Marukane S, Takagi K (2004) J Power Sources 138:253–261
40. Santee S, Xiao A, Yang L, Gnanaraj J, Lucht BL (2009) J Power Sources 194:1053–1060
41. Choi NS, Lee Y, Kim SS, Shin SC, Kang YM (2010) J Power Sources 195:2368–2371
42. Kim J, Song SW, Van Hoang H, Doh CH, Kim DW (2011) Bull Korean Chem Soc 32:105–108
43. Lewandowski A, Świderska-Mocek A, Acznik I (2010) J Appl Electrochem 40:1619–1624
44. Nadherna M, Reiter J, Moskon J, Dominko R (2011) J Power Sources 196:7700–7706